PHYSICAL REVIEW D **79,** 034018 (2009)

ϕK^+K^- production in electron-positron annihilation

S. Gómez-Avila,[1] M. Napsuciale,[1] and E. Oset[2]

[1]*Instituto de Física, Universidad de Guanajuato, Lomas del Bosque 103, Fraccionamiento Lomas del Campestre, 37150, León, Guanajuato, México*

[2]*Departamento de Física Teórica and Instituto de Física Corpuscular, Centro Mixto Universidad de Valencia-CSIC, 46000 Burjassot, Valencia, Spain*

(Received 28 November 2007; published 18 February 2009)

In this work we study the $e^+e^- \to \phi K^+K^-$ reaction. The leading order electromagnetic contributions to this process involve the $\gamma^*\phi K^+K^-$ vertex function with a highly virtual photon. We calculate this function at low energies using $R\chi PT$ supplemented with the anomalous term for the $VV'P$ interactions. Tree-level contributions involve the kaon form factors and the K^*K transition form factors. We improve this result, valid for low photon virtualities, replacing the lowest order terms in the kaon form factors and K^*K transition form factors by the form factors as obtained in $U\chi PT$ in the former case and the ones extracted from recent data on $e^+e^- \to KK^*$ in the latter case. We calculate rescattering effects which involve meson-meson amplitudes. The corresponding result is improved using the unitarized meson-meson amplitudes containing the scalar poles instead of the lowest order terms. Using the *BABAR* value for $\mathrm{BR}(X \to \phi f_0)\Gamma(X \to e^+e^-)$, we calculate the contribution from intermediate $X(2175)$. A good description of data is obtained in the case of destructive interference between this contribution and the previous ones, but more accurate data on the isovector K^*K transition form factor is required in order to exclude contributions from an intermediate isovector resonance to $e^+e^- \to \phi K^+K^-$ around 2.2 GeV.

DOI: 10.1103/PhysRevD.79.034018 PACS numbers: 13.66.Bc, 12.39.Fe, 13.60.Le, 13.75.Lb

I. INTRODUCTION

Recently, using the radiative return method [1–3], a new state, the $X(2175)$ (also named $Y(2175)$ in the literature), was observed in $e^+e^- \to \phi\pi\pi$ with the dipion invariant mass close to the $f_0(980)$ region, explicitly, for $m_{\pi\pi} =$ 850–1100 MeV [2]. Later on this state was also detected at BES in the $J/\Psi \to \eta\phi f_0(980)$ reaction [4] and BELLE in $e^+e^- \to \phi\pi^+\pi^-$ [5]. In an update of the analysis of Ref. [2], results on the channel $e^+e^- \to \phi K^+K^-$ were presented in the form of the number of events as a function of the dikaon invariant mass [3]. Indeed, in this work, the cross section for $e^+e^- \to K^+K^-K^+K^-$ was measured as a function of the center of mass energy up to $\sqrt{s} =$ 4.54 MeV and it is shown there that this reaction is dominated by events where one kaon pair comes from the decay of a ϕ. Selecting events with a kaon pair within 10 MeV of the ϕ mass, an enhancement in the invariant mass of the other kaon pair close to threshold is observed and suggested to be due to the $f_0(980)$ tail, but the low statistics and uncertainties in the $f_0(980) \to K^+K^-$ line shape prevent the authors from presenting a cross section for $e^+e^- \to \phi f_0(980)$ using the ϕK^+K^- final state.

Inspired in the physics behind the radiative $\phi \to \pi\pi\gamma$ decay [6–8], a detailed theoretical study of $e^+e^- \to \phi\pi\pi$ for pions in the s wave was performed in [9]. The process $e^+e^- \to \phi f_0$ has been also studied in the context of Nambu-Jona-Lasinio models [10]. In Ref. [9], it was shown that the tree-level contributions through the $\omega - \phi$ mixing are negligible and $e^+e^- \to \phi\pi\pi$ proceeds through the production of off-shell $K\bar{K}$ and K^*K pairs, the successive decay of the off-shell kaon or K^* into an on-shell ϕ and an off-shell K, and the subsequent $K\bar{K} \to \pi\pi$ scattering. The starting point was the $R\chi PT$ Lagrangian [11] supplemented with the anomalous term for the $V'VP$ interactions. The corresponding predictions, valid for low virtualities of the exchanged photon and low dipion invariant mass were improved in two respects. First, the s-wave $K\bar{K} \to \pi\pi$ amplitudes entering the loop calculations were replaced by the full $K\bar{K} \to \pi\pi$ isoscalar amplitudes as calculated in $U\chi PT$, which contain the scalar poles [12,13]. Second, the lowest order terms of the kaon form factor were replaced by the full kaon form factor as calculated in $U\chi PT$ [14] which describes satisfactorily the scarce data for energies around 2 GeV [15,16]. Likewise, the K^*K isoscalar transition form factor arising from $R\chi PT$ and the anomalous term, was replaced by the transition form factors as extracted from data on $e^+e^- \to K^0K^\pm\pi^\mp$ [17].

The $f_0(980)$ couples strongly to the $K\bar{K}$ system and it should contribute to the mechanisms studied in [9] in the case of $\phi K\bar{K}$ production. Therefore it is worthy to study this channel also. As discussed above, some experimental data has been released for $e^+e^- \to \phi K^+K^-$. We devote this work to the study of this reaction in the framework developed in Ref. [9]. In contrast to the $\phi\pi\pi$ final state, the ϕK^+K^- final state is induced at tree level in this framework. Furthermore, as noticed in [3], the $f_0(980)$ pole is close to the threshold for the production of the dikaon system and the loop contributions can be enhanced by this pole thus a complete analysis requires to calculate rescattering contributions. In this concern, we know that the $a_0(980)$ meson couples strongly to the K^+K^- system

but not to the $\pi\pi$ system. Therefore, in addition to the $f_0(980)$ contributions we also expect contributions from the $a_0(980)$ meson to the ϕK^+K^- final state. The $f_0(980)$ and $a_0(980)$ poles lie slightly below $2m_K$, hence their complete shapes are not expected to be seen in this reaction but their respective tails could give visible effects close to the reaction threshold. Contributions from intermediate vector mesons, $e^+e^- \to \gamma^* \to \phi V \to \phi K^+K^-$, are forbidden by charge conjugation.

An important improvement with respect to the formalism used in [9] is the more accurate characterization of the K^*K form factors. Indeed, recently, the cross section for $e^+e^- \to K^*K$ was precisely measured in the 1.7–3 GeV region [18]. We use the K^*K isoscalar and isovector transition form factors as extracted from this data in our analysis instead of the old data from [17].

The paper is organized as follows: In Sec. II we outline the calculation. Results for the tree-level contributions to $e^+e^- \to \phi K^+K^-$ are given in Sec. III. In Sec. IV we adapt previous calculations for the rescattering effects in the $\phi\pi\pi$ final state to the ϕK^+K^- final state. Section V is devoted to the extraction of the K^*K transitions form factors from data. In Sec. VI we analyze the different contributions. Section VII is devoted to estimate the intermediate $X(2175)$ contribution. Our summary and conclusions are given in Sec. VIII.

II. CALCULATION OF $e^+e^- \to \phi K^+K^-$

The calculation of the cross section for the $e^+e^- \to \phi K^+K^-$ reaction is a nontrivial task. Indeed, the leading electromagnetic contributions to this reaction are due to a single photon exchange in whose case we need to calculate the $\gamma^*\phi K^+K^-$ vertex function for a hard virtual photon ($\sqrt{s} \gtrsim 2$ GeV). This is an energy scale far beyond the well grounded calculations based on χPT, its $\mathcal{O}(p^4)$ saturated version ($R\chi PT$), or even the unitarized formalism, $U\chi PT$, which is expected to be valid up to energies of the order of 1.2 GeV; therefore it is not evident that one can perform reliable calculations at the energy of the reaction. However, whatever the responsible mechanisms for the reaction are, they must leave their fingerprint at low energies, i.e. for low photon virtualities in the $\gamma^*\phi K^+K^-$ vertex function, which can be calculated using the effective theory for QCD at low energies. We use this fact to attempt a reasonable calculation of $e^+e^- \to \phi K^+K^-$. We calculate the $\gamma^*\phi K^+K^-$ vertex function at low photon virtualities using $R\chi PT$ supplemented with the anomalous Lagrangian for the $V'VP$ interactions. As a result we obtain the electromagnetic part of the $\gamma^*\phi K^+K^-$ vertex function dominated by form factors while the pure hadronic interactions are within the scope of $R\chi PT$ in the case of tree-level contributions and involve the leading order on-shell χPT meson-meson amplitudes in the case of one-loop contributions. These results, valid at low energies, are improved using the unitarized kaon form factors (which account for the scarce experimental data at the energy of the reaction) and experimental data on the K^*K transition form factors. Similarly, the leading order on-shell meson-meson interactions are iterated following [12,13] to obtain the unitarized meson-meson amplitudes containing the scalar poles.

We start with the calculation of the tree-level contributions to $e^+e^- \to \phi K^+K^-$ within $R\chi PT$ and consider also intermediate vector meson exchange using the conventional anomalous Lagrangian for $V'VP$ interactions. We follow the conventions in [11] and the relevant interactions are given in Ref. [9]. The reaction $e^+e^- \to \phi K^+K^-$ is induced at tree level by the diagrams shown in Fig. 1. In addition to the vertices quoted in Ref. [9] there is a tree-level $\gamma\phi K^+K^-$ point interaction whose vertex is given by

$$\Gamma^{\gamma\phi K^+K^-}_{\mu\alpha\nu} = -\frac{e\sqrt{2}}{f^2}\left(G_V - \frac{F_V}{2}\right)k_\alpha g_{\mu\nu} - \frac{e\sqrt{2}G_V}{f^2}Q_\alpha g_{\mu\nu}, \tag{1}$$

with the labels $K^+(p)K^-(p')\gamma(k,\mu)\phi(Q,\alpha,\nu)$ and all incoming particles.

III. TREE-LEVEL CONTRIBUTIONS

A straightforward calculation of the set of diagrams (a) in Fig. 1 yields

$$-i\mathcal{M}^{1a} = -\frac{e^2\sqrt{2}}{f^2}\frac{L^\mu}{k^2}\Big[G_V\mathcal{T}_{\mu\nu}Q_\alpha - \left(G_V - \frac{F_V}{2}\right)g_{\mu\nu}k_\alpha\Big]\eta^{\alpha\nu}, \tag{2}$$

where $k^2 = (p^+ + p^-)^2$, $L^\mu \equiv \bar{v}(p^+)\gamma^\mu u(p^-)$. The ten-

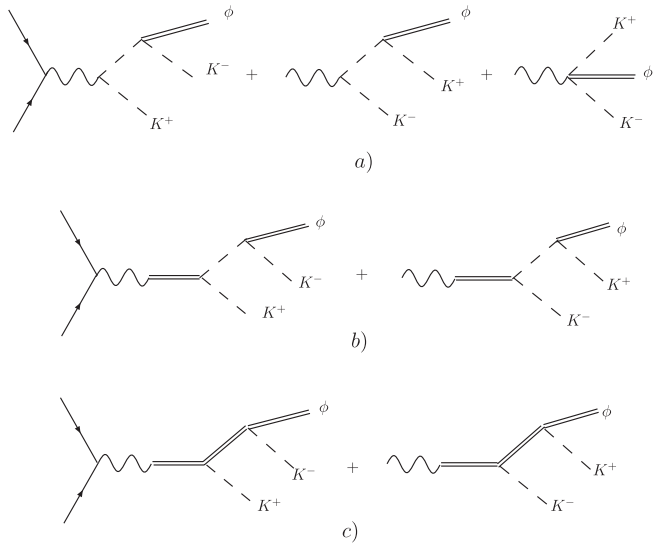

FIG. 1. Tree-level contributions to $e^+e^- \to \phi K^+K^-$: (a) pseudoscalar mesons exchange with pointlike $K^+K^-\gamma$ interaction plus contact term, (b) pseudoscalar mesons exchange with vector meson mediated $K^+K^-\gamma$ interaction, (c) intermediate vector mesons.

sor $\mathcal{T}_{\mu\nu}$ is given by

$$\mathcal{T}_{\mu\nu} = g_{\mu\nu} + \frac{(2p-k)_\mu p'_\nu}{\Box(k-p)} + \frac{(2p'-k)_\mu p_\nu}{\Box(k-p')}, \quad (3)$$

where $\Box(p) \equiv p^2 - m_K^2 + i\varepsilon$. It can be easily shown that this tensor satisfies

$$k^\mu \mathcal{T}_{\mu\nu} Q_\alpha \eta^{\alpha\nu} = 0, \quad (4)$$

where $\eta^{\alpha\nu}$ denotes the antisymmetric tensor used to describe the ϕ field in $R\chi PT$. The second term in Eq. (2) is explicitly gauge invariant, thus the $\gamma^*\phi K^+K^-$ vertex function in the amplitude (2) is gauge invariant.

Diagrams (b) in Fig. 1 involve the propagation of vector particles. These diagrams yield

$$-i\mathcal{M}^{1b} = -\frac{e^2\sqrt{2}G_V}{f^2}\frac{L^\mu}{k^2}\Big[\sum_{V=\rho,\phi,\omega}\frac{\sqrt{2}G_V F_V C_V C_{VK^+K^-}}{3f^2} \times \frac{k^2}{k^2 - M_V^2}\Big] W_{\mu\nu} Q_\alpha \eta^{\alpha\nu} \quad (5)$$

with the gauge invariant tensor

$$W_{\mu\nu} = (k^2 g_{\mu\delta} - k_\mu k_\delta)\Big(\frac{p^\delta p'_\nu}{\Box_V(k-p)} + \frac{p'^\delta p_\nu}{\Box_V(k-p')}\Big). \quad (6)$$

Using the gauge invariance property in Eq. (4) it is possible to relate this tensor to $\mathcal{T}_{\mu\nu}$ as

$$W_{\mu\nu} = \tfrac{1}{2}[k^2 \mathcal{T}_{\mu\nu} - (k^2 g_{\mu\nu} - k_\mu k_\nu)] \quad (7)$$

thus the amplitude can be rewritten as

$$-i\mathcal{M}^{1b} = -\frac{e^2\sqrt{2}G_V}{f^2}\frac{L^\mu}{k^2}\tilde{F}_{K^+}(k^2) \times \Big[\mathcal{T}_{\mu\nu} - \frac{1}{k^2}(k^2 g_{\mu\nu} - k_\mu k_\nu)\Big] Q_\alpha \eta^{\alpha\nu}, \quad (8)$$

where

$$\tilde{F}_{K^+}(k^2) = \frac{1}{2}\sum_{V=\rho,\phi,\omega}\frac{F_V}{3}\frac{\sqrt{2}G_V C_V C_{VK^+K^-}}{f^2}\frac{k^2}{k^2 - M_V^2} = \frac{G_V F_V}{2f^2}\Big(\frac{k^2}{m_\rho^2 - k^2} + \frac{1}{3}\frac{k^2}{m_\omega^2 - k^2} + \frac{2}{3}\frac{k^2}{m_\phi^2 - k^2}\Big). \quad (9)$$

Adding up contributions from diagrams (1a) and (1b) we obtain

$$-i\mathcal{M}_P = -\frac{e^2\sqrt{2}G_V}{f^2}\frac{L^\mu}{k^2}\Big[F_{K^+}^{VMD}(k^2)\mathcal{T}_{\mu\nu} - \tilde{F}_{K^+}(k^2)\frac{1}{k^2} \times (k^2 g_{\mu\nu} - k_\mu k_\nu)\Big] Q_\alpha \eta^{\alpha\nu} + \frac{e^2\sqrt{2}}{f^2}\Big(G_V - \frac{F_V}{2}\Big)\frac{L^\mu}{k^2} g_{\mu\nu} k_\alpha \eta^{\alpha\nu}, \quad (10)(11)$$

where

$$F_{K^+}^{\rm VMD}(k^2) = 1 + \tilde{F}_{K^+}(k^2) = 1 + \frac{G_V F_V}{2f^2}\Big(\frac{k^2}{m_\rho^2 - k^2} + \frac{1}{3}\frac{k^2}{m_\omega^2 - k^2} + \frac{2}{3}\frac{k^2}{m_\phi^2 - k^2}\Big). \quad (12)$$

Notice that the second term in Eq. (10) contains the vector meson contributions to the kaon form factor, but the constant term due to the electric charge is missing. A similar result was obtained in [9]. This term should come from Lagrangians with higher derivatives of the fields, specifically from the term $\partial^\alpha V_{\alpha\nu}\partial_\mu f_+^{\mu\nu}$, which is absent in our basic interactions. We will assume in the following that the constant term due to the charge is provided by such missing interactions; hence, we will write $F_{K^+}^{\rm VMD}$ instead of $\tilde{F}_{K^+}$ in the second term of Eq. (10). Also, notice that the function $F_{K^+}^{\rm VMD}(k^2)$ accounts for the lowest order terms of the charged kaon form factor and describes it properly at low k^2. The high virtuality of the exchanged photon in our process requires to work out the complete γK^+K^- vertex function. The calculation of the kaon form factors has been done in the context of $U\chi PT$ in Ref. [14]. Although this calculation misses the contributions of the first radially excited vector mesons which are important around 1.7 GeV, the existing experimental data close to the $\phi K\bar{K}$ threshold are properly described by the unitarized kaon form factors as shown in Fig. 2 where the results for the unitarized charged kaon form factor are plotted together with data from the DM2 Collaboration [15]. Thus in the following we will replace the lowest order terms so far obtained, $F_{K^+}^{\rm VMD}(k^2)$, by the full unitarized form factor $F_{K^+}(k^2)$. In addition to the terms associated to the kaon

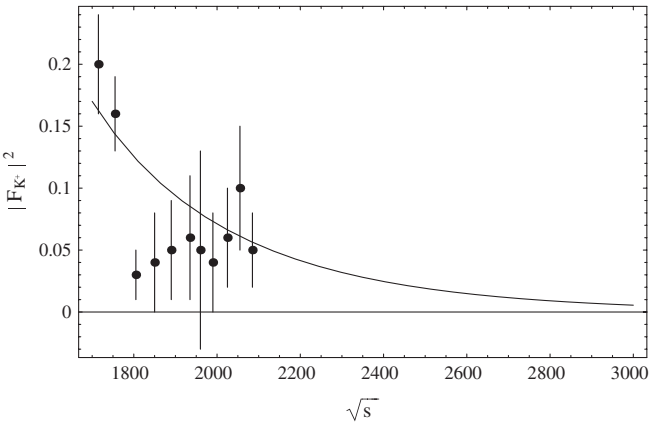

FIG. 2. Unitarized charged kaon form factor. Experimental points are taken from Ref. [15].

form factor we get a contact term with the combination $G_V - \frac{F_V}{2}$. This combination is small and it vanishes in the context of vector meson dominance [19]. Clearly, this term cannot be extrapolated to high photon virtualities without its dressing by a form factor. The impact of this term on the cross section for the $\phi\pi\pi$ final state upon its dressing with the kaon form factors was found to be very small in [9]. Its contribution turns out to be small also in this case when it is dressed with the charged kaon form factor, thus we will skip it in the following. With these considerations the amplitude reads

$$-i\mathcal{M}_P = -\frac{e^2\sqrt{2}G_V}{f^2}\frac{L^\mu}{k^2}F_{K^+}(k^2) \times\left[\mathcal{T}_{\mu\nu} - \frac{1}{k^2}(k^2 g_{\mu\nu} - k_\mu k_\nu)\right]Q_\alpha \eta^{\alpha\nu}. \quad (13)$$

In terms of the conventional polarization vector η^ν satisfying

$$Q_\alpha \eta^{\alpha\nu}(Q) = iM_\phi \eta^\nu(Q),$$
$$g_{\mu\nu}k_\alpha \eta^{\alpha\nu}(Q) = \frac{i}{M_\phi}(Q\cdot k g_{\mu\nu} - Q_\mu k_\nu)\eta^\nu(Q), \quad (14)$$

we finally obtain the tree-level contribution from the exchange of pseudoscalar mesons as

$$-i\mathcal{M}_P = -\frac{ie^2\sqrt{2}G_V M_\phi}{f^2}\frac{L^\mu}{k^2}F_{K^+}(k^2)\left[\mathcal{T}_{\mu\nu} - \frac{1}{k^2} \times (k^2 g_{\mu\nu} - k_\mu k_\nu)\right]\eta^\nu. \quad (15)$$

The amplitude for the diagrams (c) in Fig. 1 is

$$-i\mathcal{M}^{1c} = -\frac{e^2 G_T}{\sqrt{2}}\left(\frac{M_{K^*}}{16}\right)F^{lo}_{K^{*+}K^-}(k^2)\frac{L^\mu}{k^2}R_{\mu\alpha\nu}\eta^{\alpha\nu}. \quad (16)$$

Here, we get the $K^{*+}K^-$ transition form factor to leading order as

$$F^{lo}_{K^{*+}K^-}(k^2) = \sum_{V=\rho,\omega.\phi}\frac{G_T C_{VK^{*+}K^-}}{\sqrt{2}}\frac{F_V C_V}{3M_{K^*}}\frac{1}{k^2 - M_V^2} = \frac{F_V G}{6}\left(\frac{M_\omega}{k^2 - M_\omega^2} + \frac{3M_\rho}{k^2 - M_\rho^2} - \frac{2M_\phi}{k^2 - M_\phi^2}\right), \quad (17)$$

and $R_{\mu\alpha\nu}$ stands for the tensor

$$R_{\mu\alpha\nu} = g_{\mu\beta}k_\sigma \Delta^{\sigma\beta\gamma\delta}(k)\epsilon_{\gamma\delta\phi\eta}\left[\frac{\Delta^{\phi\eta\sigma\tau}(k-p)}{\Box_{K^*}(k-p)} + \frac{\Delta^{\phi\eta\sigma\tau}(k-p')}{\Box_{K^*}(k-p')}\right]\epsilon_{\sigma\tau\alpha\nu}, \quad (18)$$

with $\Box_{K^*}(p) = p^2 - m^2_{K^*}$, which is explicitly gauge invariant. It can be shown that

$$R_{\mu\alpha\nu}\eta^{\alpha\nu} = \frac{16i}{M_\phi M_{K^*}}\mathcal{V}_{\mu\nu}\eta^\nu, \quad (19)$$

where

$$\mathcal{V}_{\mu\nu} = k^\delta \epsilon_{\mu\delta\phi\eta}\left[\epsilon^{\phi\eta}{}_{\alpha\nu} + \epsilon_\sigma{}^\phi{}_{\alpha\nu}\left(\frac{(k-p)^\eta(k-p)^\sigma}{\Box_{K^*}(k-p)} + \frac{(k-p')^\eta(k-p')^\sigma}{\Box_{K^*}(k-p')}\right)\right]Q^\alpha. \quad (20)$$

The amplitude in Eq. (16) contains the leading order terms for the $K^{*+}K^-$ transition form factor valid for low photon virtualities. The photon exchanged in $e^+e^- \to \phi K^+K^-$ has $k^2 \gtrsim 2$ GeV and we should work out this form factor for such high photon virtualities. In the numerical computations we replace the leading order terms by the complete transition form factor, $F_{K^{*+}K^-}(k^2)$, extracted from recent data on $e^+e^- \to K^0K^\pm\pi^\mp$, $K^+K^-\pi^0$ to be discussed below. With these considerations

$$-i\mathcal{M}^{1c} = -\frac{ie^2 G}{\sqrt{2}}F_{K^{*+}K^-}(k^2)\frac{L^\mu}{k^2}\mathcal{V}_{\mu\nu}\eta^\nu. \quad (21)$$

IV. RESCATTERING EFFECTS

The final state ϕK^+K^- can get contributions from the $K^+K^- \to K^+K^-$ rescattering. Furthermore, this final state can also be reached through the production of $\phi K^0\bar{K}^0$ and the rescattering $K^0\bar{K}^0 \to K^+K^-$. Excitation of higher mass states such as K^*K is also possible and the final state ϕK^+K^- can be produced by the initial production of an off-shell $K^{*0}\bar{K}^0$ ($K^{*+}K^-$) pair, the subsequent decay of the off-shell K^{*0} (K^{*+}) into a $\phi K^0(\phi K^+)$, and the rescattering $K^0\bar{K}^0 \to K^+K^-$ ($K^+K^- \to K^+K^-$). This section is devoted to the study of these contributions.

We calculate the rescattering effects to lowest order in the chiral expansion from $R\chi PT$ supplemented with the anomalous term for the $V'VP$ interactions. These results are improved by the unitarization of meson-meson amplitudes proposed in [12] which dynamically generates the scalar resonances. The relevant diagrams in $R\chi PT$ are shown in Fig. 3, where for simplicity a shaded circle and a dark circle account for the diagrams (i) plus (j) and (k) plus (l), respectively, which differentiate the direct photon coupling from the coupling through an intermediate vector meson.

The factorization of the meson-meson chiral amplitudes on shell out of the loop integrals has been discussed in [9] in the case of the $\phi\pi\pi$ final state. The same considerations apply to the ϕK^+K^- final state and we refer the reader to Ref. [9] for the details. To account for the whole rescattering effects in $K^+K^- \to K^+K^-$ and $K^0\bar{K}^0 \to K^+K^-$ in these diagrams we iterate the lowest order chiral amplitudes in the scalar channel, $V_{K^+K^+}$ and $V_{K^0K^+}$ to obtain the unitarized scalar amplitudes, $t_{K^+K^+}$ and $t_{K^0K^+}$ (in the following we skip the suffix ^{0} used in [9] for the scalar meson-

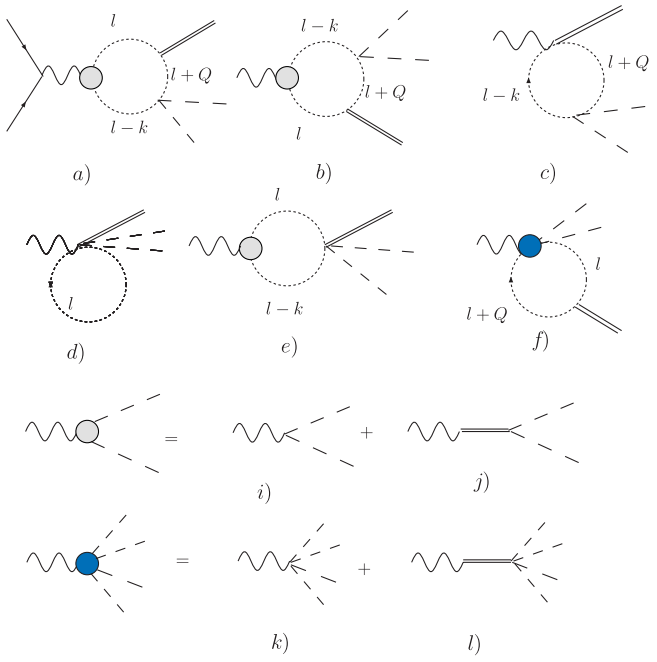

FIG. 3 (color online). Feynman diagrams for $e^+e^- \to \phi K^+K^-$ in $R\chi PT$ at one-loop level.

meson amplitudes in order to handle isospin labels that will be necessary below and denote $t^I_{MM'}$ the $M\bar{M} \to M'\bar{M}'$ unitarized amplitude in the isospin channel I). Unlike the $\phi\pi\pi$ case where only the isoscalar meson-meson unitarized amplitude containing the $f_0(980)$ pole is involved, in the case of the ϕK^+K^- final state the necessary $t_{K^+K^+}$ and $t_{K^0K^+}$ amplitudes are linear combinations of the isoscalar and isovector scalar amplitudes t^0_{KK} and t^1_{KK}. The last one contains the $a_0(980)$ pole. Notice that we are using the scalar amplitudes $t_{K^+K^+}$ and $t_{K^0K^+}$ instead of the full amplitudes which in principle contain higher angular momentum contributions. This is expected to be a good approximation for energies near the reaction threshold due to the small trimomentum of the dikaon system. Furthermore, at these energies the dikaon mass is near the $f_0(980)$ and $a_0(980)$ poles and the p-wave amplitudes (containing vector poles) give vanishing contribution to this process due to charge conjugation. Higher l (tensor) contributions are expected to be important at much higher center of mass energy. The dominance of s waves near threshold has been observed in alike processes as $J/\psi \to VPP$ [20].

The loop calculations go similarly to those of the $\phi\pi\pi$ final state done in Ref. [9]. We adopt the same convention of all external particles incoming and refer the reader to that work for the details. For kaons in the loops we obtain

$$-i\mathcal{M}_K = \frac{-ie^2}{2\pi^2 m_K^2}\frac{L^\mu}{k^2}[A_P L^{(1)}_{\mu\nu} + B_P L^{(2)}_{\mu\nu}]\eta^\nu \tag{22}$$

with the Lorentz structures

$$L^{(1)}_{\mu\nu} \equiv Q\cdot k g_{\mu\nu} - Q_\mu k_\nu, \qquad L^{(2)}_{\mu\nu} = k^2 g_{\mu\nu} - k_\mu k_\nu, \tag{23}$$

and

$$A_P = \frac{\sqrt{2}M_\phi G_V}{2f^2}[t_{K^+K^+}F_{K^+}(k^2) + t_{K^0K^+}F_{K^0}(k^2)]I_P, \tag{24}$$

$$B_P = \frac{\sqrt{2}M_\phi G_V}{2f^2}[t_{K^+K^+}F_{K^+}(k^2) + t_{K^0K^+}F_{K^0}(k^2)] \times \left(J_P + \frac{m_K^2}{4k^2}g_K\right). \tag{25}$$

The loop functions are given by

$$I_P = \int_0^1 dx \int_0^x dy \times \frac{y(1-x)}{1 - \frac{Q^2}{m_K^2}x(1-x) - \frac{2Q\cdot k}{m_K^2}(1-x)y - \frac{k^2}{m_K^2}y(1-y) - i\varepsilon}, \tag{26}$$

$$J_P = \frac{1}{2}\int_0^1 dx \int_0^x dy \times \frac{y(1-2y)}{1 - \frac{Q^2}{m_K^2}x(1-x) - \frac{2Q\cdot k}{m_K^2}(1-x)y - \frac{k^2}{m_K^2}y(1-y) - i\varepsilon}, \tag{27}$$

$$g_K = -1 + \log\frac{m_K^2}{\mu^2} + \sigma\log\frac{\sigma+1}{\sigma-1}, \tag{28}$$

with $\sigma = \sqrt{1 - 4m_K^2/m_{KK}^2}$. Notice that the only change from the final $\phi\pi^+\pi^-$ state [9], to the present case, is the substitution of the factor $t_{K^+\pi^+}F_{K^+}(k^2) + t_{K^0\pi^+}F_{K^0}(k^2)$ by $t_{K^+K^+}F_{K^+}(k^2) + t_{K^0K^+}F_{K^0}(k^2)$. It is convenient to write the meson-meson scalar amplitudes in isospin basis. With the conventions in Refs. [12,14], we get

$$t_{K^+K^+} = \tfrac{1}{2}(t^0_{KK} + t^1_{KK}), \qquad t_{K^0K^+} = \tfrac{1}{2}(t^0_{KK} - t^1_{KK}), \tag{29}$$

thus, in terms of the isoscalar (t^0_{KK}, $F^0_K(k^2)$) and isovector (t^1_{KK}, $F^1_K(k^2)$) meson-meson amplitudes and kaon form factors, respectively, we obtain

$$A_P = \frac{M_\phi G_V}{2\sqrt{2}f^2}[t^0_{KK}F^0_K(k^2) + t^1_{KK}F^1_K(k^2)]I_P, \tag{30}$$

$$B_P = \frac{M_\phi G_V}{2\sqrt{2}f^2}[t^0_{KK}F^0_K(k^2) + t^1_{KK}F^1_K(k^2)]\left(J_P + \frac{m_K^2}{4k^2}g_K\right), \tag{31}$$

with the isoscalar and isovector form factors

$$F_K^0(k^2) = F_{K^+}(k^2) + F_{K^0}(k^2),$$
$$F_K^1(k^2) = F_{K^+}(k^2) - F_{K^0}(k^2). \tag{32}$$

Similarly to the tree-level contributions, the calculation of kaon loops yields also a contact term with the combination $G_V - \frac{F_V}{2}$ not shown in Eq. (22). For the same reasons we neglected the analogous term in the previous section, we will also neglect it here.

The process $e^+e^- \to \phi K^+K^-$ can also proceed through the diagrams shown in Fig. 4. Again, the calculations are similar to the case of $\phi\pi\pi$ in the final state calculated in Ref. [9] and we refer to this work for details on the notation and conventions. The amplitude from the diagram in Fig. 4 gets contributions from charged and neutral K^*K in the loops. We obtain the amplitude from these diagrams as

$$-i\mathcal{M}_V = \frac{-ie^2}{2\pi^2 m_K^2}\frac{L^\mu}{k^2}[A_V L^{(1)}_{\mu\nu} + B_V L^{(2)}_{\mu\nu}]\eta^\nu \tag{33}$$

with

$$A_V = \frac{G}{4\sqrt{2}}[F_{K^{*+}K^-}(k^2)t_{K^+K^+} + F_{K^{*0}\bar{K}^0}(k^2)t_{K^0K^+}]I_V, \tag{34}$$

$$B_V = -\frac{GM_\phi^2}{4\sqrt{2}}[F_{K^{*+}K^-}(k^2)t_{K^+K^+} + F_{K^{*0}\bar{K}^0}(k^2)t_{K^0K^+}]J_V, \tag{35}$$

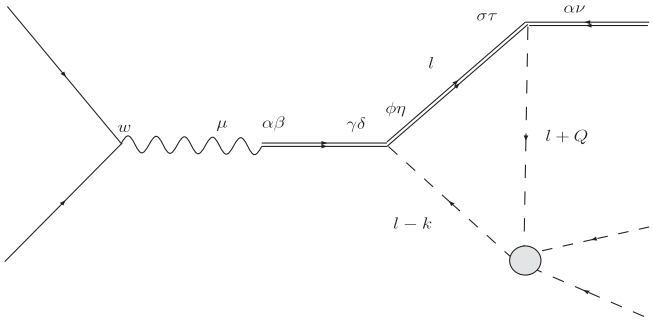

FIG. 4. Feynman diagram for rescattering effects in $e^+e^- \to K^*\bar{K} \to \phi K\bar{K} \to \phi K^+K^-$.

$$I_V = m_K^2\left(I_G - I_2 + 2 + \frac{1}{2}\log\frac{m_K^2}{\mu^2}\right) + Q\cdot k J_V. \tag{36}$$

Here $F_{K^{*+}K^-}(k^2)$ stands for the leading order terms in the $K^{*+}K^-$ transition form factor in Eq. (17) and $F_{K^{*0}\bar{K}^0}(k^2)$ denotes the $K^{*0}\bar{K}^0$ leading order terms of the neutral transition form factor given by

$$F_{K^{*0}\bar{K}^0}(k^2) = \frac{F_V G}{6}\left(\frac{M_\omega}{k^2 - M_\omega^2} - \frac{3M_\rho}{k^2 - M_\rho^2} - \frac{2M_\phi}{k^2 - M_\phi^2}\right). \tag{37}$$

The loop functions are given by

$$J_V = \int_0^1 dx \int_0^x dy \frac{y(1-x)}{1 - \frac{Q^2}{m_K^2}x(1-x) - \frac{2Q\cdot k}{m_K^2}(1-x)y - \frac{k^2}{m_K^2}y(1-y) - \frac{(m_{K^*}^2 - m_K^2)}{m_K^2}(y-x) - i\varepsilon}, \tag{38}$$

$$I_2 = \int_0^1 dx \int_0^x dy \log\left[1 - \frac{Q^2}{m_K^2}x(1-x) - \frac{2Q\cdot k}{m_K^2}(1-x)y - \frac{k^2}{m_K^2}y(1-y) - \frac{(m_{K^*}^2 - m_K^2)}{m_K^2}(y-x) - i\varepsilon\right], \tag{39}$$

$$I_G = -2 + \log\frac{m_K^2}{\mu^2} + \sigma\log\frac{\sigma+1}{\sigma-1}. \tag{40}$$

Notice again that the only change from the final $\phi\pi^+\pi^-$ state to the present case is the replacement of the factor $t_{K^+\pi^+}F_{K^{*+}K^-}(k^2) + t_{K^0\pi^+}F_{K^{*0}\bar{K}^0}(k^2)$ by $t_{K^+K^+}F_{K^{*+}K^-}(k^2) + t_{K^0K^+}F_{K^{*0}\bar{K}^0}(k^2)$. In terms of the isoscalar and isovector amplitudes and transition form factors we get

$$A_V = \frac{G}{8\sqrt{2}}[t^0_{KK}F^0_{K^*K}(k^2) + t^1_{KK}F^1_{K^*K}(k^2)]I_V,$$
$$B_V = -\frac{GM_\phi^2}{8\sqrt{2}}[t^0_{KK}F^0_{K^*K}(k^2) + t^1_{KK}F^1_{K^*K}(k^2)]J_V, \tag{41}$$

with

$$F^0_{K^*K}(k^2) = F_{K^{*+}K^-}(k^2) + F_{K^{*0}\bar{K}^0}(k^2),$$
$$F^1_{K^*K}(k^2) = F_{K^{*+}K^-}(k^2) - F_{K^{*0}\bar{K}^0}(k^2). \tag{42}$$

Finally, taking into account both pseudoscalars [Eq. (22)] and vectors [Eq. (33)] in the loops we obtain the total amplitude as

$$-i\mathcal{M} = \frac{-ie^2}{2\pi^2 m_K^2}\frac{L^\mu}{k^2}[AL^{(1)}_{\mu\nu} + BL^{(2)}_{\mu\nu}]\eta^\nu, \tag{43}$$

where

$$A = A_P + A_V, \qquad B = B_P + B_V \tag{44}$$

with the specific functions in Eqs. (30), (31), and (41). Recall these results are valid for ingoing particles. For the numerical computations in the following section we reverse the momenta of the final particles to obtain

$$-i\mathcal{M}_L = \frac{ie^2}{2\pi^2 m_K^2}\frac{L^\mu}{k^2}[IL^{(1)}_{\mu\nu} - JL^{(2)}_{\mu\nu}]\eta^\nu \tag{45}$$

with

$$I = \tilde{A}_P - \tilde{A}_V, \qquad J = \tilde{B}_P - \tilde{B}_V, \tag{46}$$

where the functions $\tilde{A}_P$, $\tilde{A}_V$, $\tilde{B}_P$, $\tilde{B}_V$ are obtained from the untilded functions in Eqs. (30), (31), and (41) just changing the sign of $Q \cdot k$ in the integrals I_P, J_P, J_V, and I_2 in Eqs. (26), (27), (38), and (39).

V. K^*K TRANSITION FORM FACTORS

Our results involve the K^*K isoscalar and isovector transition form factors at the center of mass energy of the reaction. Our calculation based on Lagrangians suitable for low energies yields the lowest order terms in the chiral expansion for these form factors. Since a calculation of these form factors at such huge energies as $\sqrt{s} \geq 2$ GeV is beyond the scope of the effective theories used here, we consider our calculation as a convenient procedure to identify the main physical effects (form factors and meson-meson amplitudes) and must find a way to enlarge the range of validity of the calculation to high energies. We do this by replacing the leading order terms in the transition form factors by an appropriate characterization of these form factors at the energy of the reaction. In the case of the $\phi\pi\pi$ final state, only the isoscalar transition form factor is required and in [9] it was extracted from data on $e^+e^- \to K\bar{K}\pi$, at $\sqrt{s} = 1400$–2180 MeV reported in [17]. In the present case, also the isovector transition form factor is required. This form factor cannot be extracted from this data due to the low statistics. Indeed, in [17] it is assumed that the isovector amplitude is dominated by a ρ' with a mass and width fixed to $m_{\rho'} = 1570$ MeV and $\Gamma_{\rho'} = 510$ MeV in the interpretation of the data. Fortunately, high precision measurements for the cross section of $e^+e^- \to K^+K^-\pi^0$, $K^0K^\pm\pi^\mp$ were recently released where the contributions from intermediate K^* are identified [18]. The first reaction involves the charged K^*K transition form factor while the second gets contributions of both charged and neutral transition form factors. Using this data, the isoscalar and isovector components of the cross section for $e^+e^- \to K^*K$ at $\sqrt{s} =$ 1400–3000 MeV were extracted along with an energy dependent phase which signals another resonance below 2 GeV which could not be resolved [18].

We extract the form factors from this data as follows. First we calculate the $\gamma(k, \mu)K^*(q, \nu)K(p)$ vertex function in $R\chi PT$ and replace the lowest order terms in the transition form factor by the full one to obtain

$$\Gamma_{\mu\nu}(k, q) = ieF_{K^*K}(k^2)\epsilon_{\mu\nu\alpha\beta}k^\alpha q^\beta \tag{47}$$

with all incoming particles. A straightforward calculation of the $e^+e^- \to K^*K$ cross section using this effective vertex yields

$$\sigma(s) = \frac{\pi\alpha^2}{6s^3}|F_{K^*K}(s)|^2\lambda^{3/2}(s, m_{K^*}^2, m_K^2), \tag{48}$$

where

$$\lambda(m_1^2, m_2^2, m_3^2) = (m_1^2 - (m_2 - m_3)^2)(m_1^2 - (m_2 + m_3)^2). \tag{49}$$

In Ref. [18] a fit was done to the isovector and isoscalar components of $e^+e^- \to K^+K^-\pi^0$, $K^0K^\pm\pi^\mp$ using also data on the cross section for the production of $\phi\eta$ where the ϕ' peak is visible. The analysis below 2 GeV required the introduction of an energy dependent relative phase pointing to the existence of an unresolved resonance in this energy region, in addition to the ρ' and the ϕ'. Here, we are interested only in an appropriate characterization of the isoscalar and isovector form factors in the 2–3 GeV region where the effect of this phase should be small. The experimental points for the squared absolute value of the form factors are obtained using Eq. (48) and Tables VI and VII of Ref. [18]. Physically, these form factors are dominated by the exchange of resonances; hence in their characterization we complement the lowest order terms obtained in $R\chi PT$ with the exchange of heavy mesons

$$F^0_{K^*K}(k^2) = \frac{F_V G}{3}\left(\frac{M_\omega}{k^2 - M_\omega^2} - \frac{2M_\phi}{k^2 - M_\phi^2}\right) + b_0\left(\frac{-2m_{\phi'}^2}{k^2 - m_{\phi'}^2 + i\sqrt{s}\Gamma_{\phi'}(s)}\right), \tag{50}$$

$$F^1_{K^*K}(k^2) = \frac{F_V G}{3}\left(\frac{3m_\rho}{k^2 - m_\rho^2}\right) + b_1\left(\frac{3m_{\rho'}^2}{k^2 - m_{\rho'}^2 + i\sqrt{s}\Gamma_{\rho'}(s)}\right), \tag{51}$$

with the energy dependent widths used in [18]

$$\Gamma_{\phi'}(s) = \Gamma_{\phi'}\left[\frac{\mathcal{P}_{K^*K}(s)}{\mathcal{P}_{K^*K}(m_{\phi'}^2)}B_{KK^*}^{\phi'} + \frac{\mathcal{P}_{\phi\eta}(s)}{\mathcal{P}_{\phi\eta}(m_{\phi'}^2)}B_{\phi\eta}^{\phi'} + (1 - B_{KK^*}^{\phi'} - B_{\phi\eta}^{\phi'})\right],$$

$$\Gamma_{\rho'}(s) = \Gamma_{\rho'}\left[\frac{\mathcal{P}_{4\pi}(s)}{\mathcal{P}_{4\pi}(m_{\rho'}^2)}B_{4\pi}^{\rho'} + (1 - B_{4\pi}^{\rho'})\right],$$

where

$$\mathcal{P}_{VP}(s) = \left(\frac{\lambda(s, m_V^2, m_P^2)}{s}\right)^{3/2}, \qquad \mathcal{P}_{4\pi}(s) = \frac{(s - 16m_\pi^2)^{3/2}}{s}. \tag{52}$$

The values for the constants appearing here are extracted from the central values of Table XV in [18] as $B_{KK^*}^{\phi'} = 0.5$, $B_{\phi\eta}^{\phi'} = 0.20$, $B_{4\pi}^{\rho'} = 0.65$, $m_{\phi'} = 1723$ MeV, $\Gamma_{\phi'} =$ 371 MeV, $m_{\rho'} = 1504$ MeV, $\Gamma_{\rho'} = 438$ MeV. The parameters b_0, b_1 are fitted to the data for the isoscalar and isovector cross sections reported in Tables VI and VII of [18], respectively. The fit to the isoscalar cross section

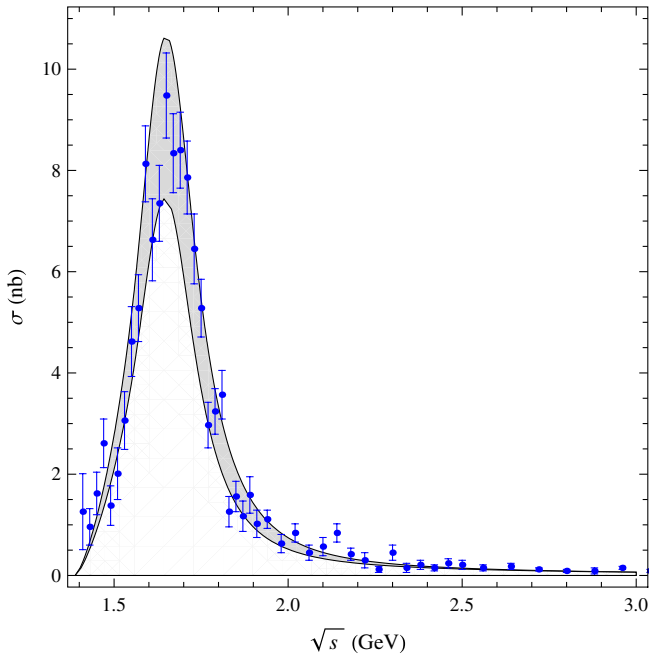

FIG. 5 (color online). Cross section for $e^+e^- \to K^*K$ in the isoscalar channel. The band corresponds to the 1σ region of our parametrization of the form factors in Eq. (50). Data points are taken from Table VI of Ref. [18].

yields $b_0 = -0.2487 \times 10^{-3}$ MeV^{-1}. The fit to the isovector cross section yields $b_1 = -0.2551 \times 10^{-3}$ MeV^{-1}.

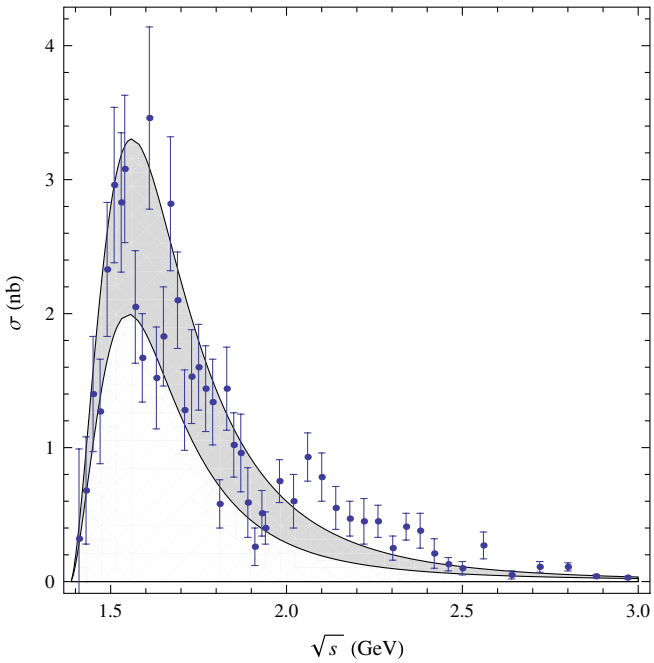

FIG. 6 (color online). Cross section for $e^+e^- \to K^*K$ in the isovector channel. The band corresponds to the 1σ region of the parametrization of the form factors in Eq. (51). Data points are taken from Table VII of Ref. [18].

Notice that these values are nearly equal, pointing to the ϕ' and ρ' as members of an $SU(3)$ nonet. Our results for the corresponding cross sections are shown in Figs. 5 and 6, where the shadowed bands correspond to the 1σ regions for the parameters b_0 and b_1. A good description of the isoscalar cross section is obtained but more accurate data on the isovector $e^+e^- \to K^*K$ cross section is desirable. The discrepancy in this case is due to the effects of another intermediate resonance around $\sqrt{s} = 2$ GeV in $e^+e^- \to K^*K$ which, however, could not be resolved in [18].

As a cross check, we calculate the full cross section for $e^+e^- \to K^+K^-\pi^0$ from the exchange of K^* which involves only the charged transition form factor and obtain a proper description of data in Table III of Ref. [18] up to $\sqrt{s} = 3$ GeV.

VI. NUMERICAL RESULTS AND DISCUSSION

With respect to the $\phi\pi\pi$ production with s-wave pions studied in [9], there is now the novelty of the tree-level contributions in ϕK^+K^- production with K^+K^- pairs in all possible angular momentum states. In the case of loops, our calculations consider only s-wave K^+K^- in the final state because we are using the unitarized amplitudes for $K\bar{K} \to K^+K^-$ which per construction are projected onto well defined angular momentum ($l = 0$) and isospin ($I = 0, 1$). In the appendix we give details on the integration of phase space and state our conventions. The dikaon spectrum turns out to be

$$\frac{d\sigma}{dm_{KK}} = \frac{1}{(2\pi)^4}\frac{m_{KK}}{16s^{3/2}} \times \int_{E_-}^{E_+} dE \int_0^{\pi} d\cos\theta_V \int_0^{2\pi} d\varphi |\bar{\mathcal{M}}|^2, \quad (53)$$

where

$$\mathcal{M} = \mathcal{M}_P + \mathcal{M}^{1c} + \mathcal{M}_L \quad (54)$$

and these amplitudes are given in Eqs. (15), (21), and (45), respectively. We refer the reader to the appendix for further details on the notation and integration of phase space. We evaluate numerically the integrals and the differential cross section using the physical masses and coupling constants. We remark that all the parameters entering this calculation have been fixed in advance and, in this sense, there are no free parameters. In our numerical analysis we use $m_K = 495$, $m_\phi = 1019.4$, $\alpha = 1/137$, $G_V = 53$ MeV, $F_V = 154$ MeV, $f_\pi = 93$ MeV, and $G = 0.016$ MeV^{-1}. Concerning the rescattering effects we remark that the $K^+K^- \to K^+K^-$ and $K^0\bar{K}^0 \to K^+K^-$ scattering between the kaons in the loops and the final kaons takes place at the dikaon invariant mass independently of the value of $\sqrt{s}$ and of the momenta in the loops. As a consequence, when replacing the lowest order terms for this amplitude by the unitarized amplitude, we can safely use the results of [12,13] and take a renormalization scale $\mu = 1.2$ GeV

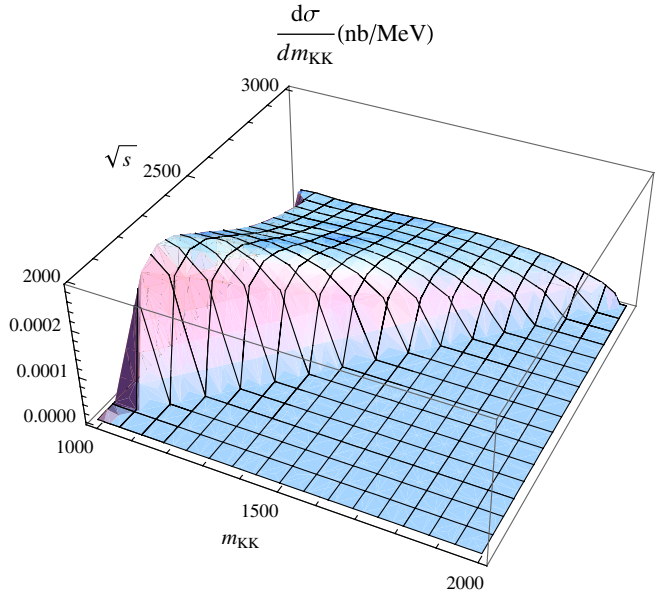

FIG. 7 (color online). Dikaon spectrum as a function of the center of mass energy.

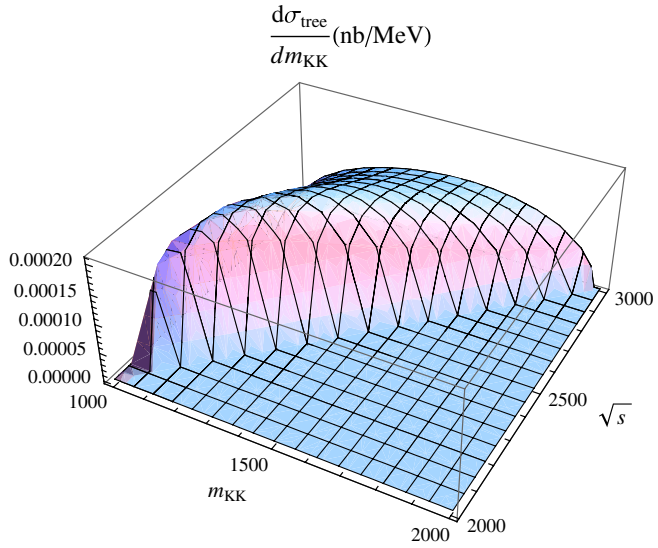

FIG. 9 (color online). Dikaon spectrum as a function of the center of mass energy for the tree-level contributions.

for the function G_K [13], in spite of the fact that the reaction $e^+e^- \to \phi K^+K^-$ takes place at a much higher energy $\sqrt{s} \geq 2$ GeV. The unitarized amplitudes naturally contain the scalar poles and there is no need to include explicitly these degrees of freedom in the calculation. We obtain the dikaon spectrum shown in Fig. 7 for $\sqrt{s} =$ 2010–3000 MeV. In order to compare with the dikaon spectrum in Fig. 26 of [3], we should collect all events from threshold up to $\sqrt{s} = 4.5$ GeV as included in the sample for that figure. This amounts to integrate our differential cross section on $\sqrt{s}$ in this energy range. Although a precise comparison cannot be carried out since data is presented in the form of a number of events, our results in Fig. 8 follow a similar pattern to those of Fig. 26 of [3]. In order to check the conjecture in [3] that the enhancement close to the dikaon threshold in the integrated spectrum is due to the presence of the $f_0(980)$ pole, in this plot we also show the individual contributions coming from tree level and rescattering. The dashed plots are obtained integrating on $\sqrt{s}$ the tree level and rescattering individual contributions to the dikaon spectrum at different $\sqrt{s}$ shown in Figs. 9 and 10. The analogous spectrum for the interference between tree-level and rescattering contributions is shown in Fig. 11.

The enhancement near threshold for rescattering effects in Fig. 10 is due to the tails of the $f_0(980)$ and the $a_0(980)$ whose poles are well reproduced in the unitarization of

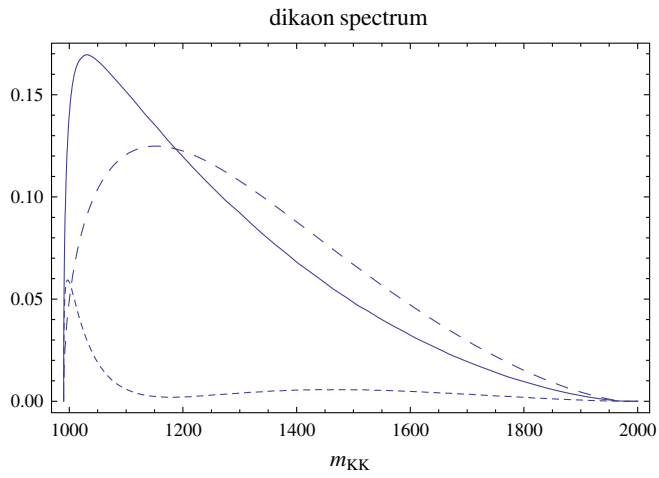

FIG. 8 (color online). Integrated dikaon mass spectrum for tree-level (long-dashed line), rescattering (short-dashed line), and total (solid line) contributions.

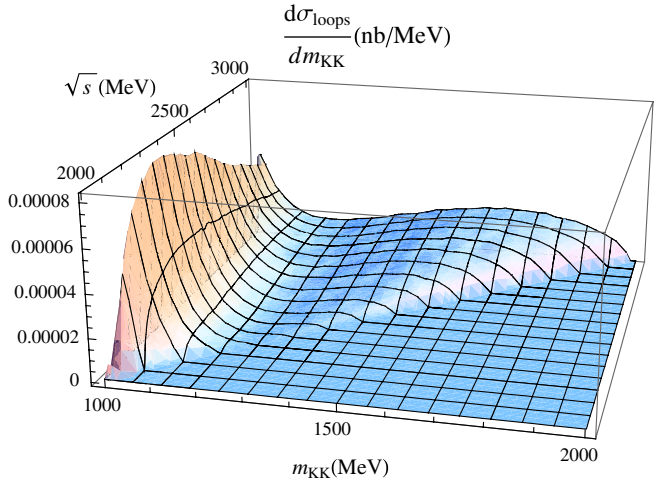

FIG. 10 (color online). Dikaon spectrum of the contributions coming from rescattering as a function of the dikaon invariant mass for different values of the center of mass energy.

meson-meson s-wave amplitudes present in our calculation. In contrast to the $\phi\pi\pi$ final state studied in [9] where the complete $f_0(980)$ resonance is visible in the dipion spectrum, here the peaks of both f_0 and a_0 lie below $2m_K$ in the dikaon invariant mass, i.e. below the threshold for the production of the dikaon system in the reaction $e^+e^- \to \phi K^+K^-$, thus, it is only the tail of these resonances that the kinematics allows us to see.

Close to the threshold for the dikaon production, rescattering effects are enhanced by the scalar poles. However, the integrated spectrum in Fig. 8 shows that these contributions are of the same order as tree-level ones close to threshold only. Beyond this region tree-level contributions become dominant. We can also see a constructive interference between these contributions close to threshold and a destructive interference beyond $m_{KK} = 1200$ MeV in the integrated dikaon spectrum.

A closer analysis of tree-level contributions shows that they are dominated by the exchange of K^*, thus the enhancement close to threshold in the integrated dikaon spectrum in Fig. 8 is due to both the scalar poles and tree-level K^* exchange. Events beyond threshold are mainly due to K^* exchange at tree level.

The interference is more transparent at the level of the dikaon spectrum as a function of $\sqrt{s}$ shown in Fig. 11. The sign depends both on m_{KK} and $\sqrt{s}$ but for a fixed $\sqrt{s}$ it is positive close to the dikaon threshold and evolves to a negative interference beyond this threshold. This interference shows up differently in the total cross section for $e^+e^- \to \phi K^+K^-$ obtained upon integration of the dikaon invariant mass in Fig. 7. Our result for the cross section is shown in Fig. 12. Here, we get a constructive interference

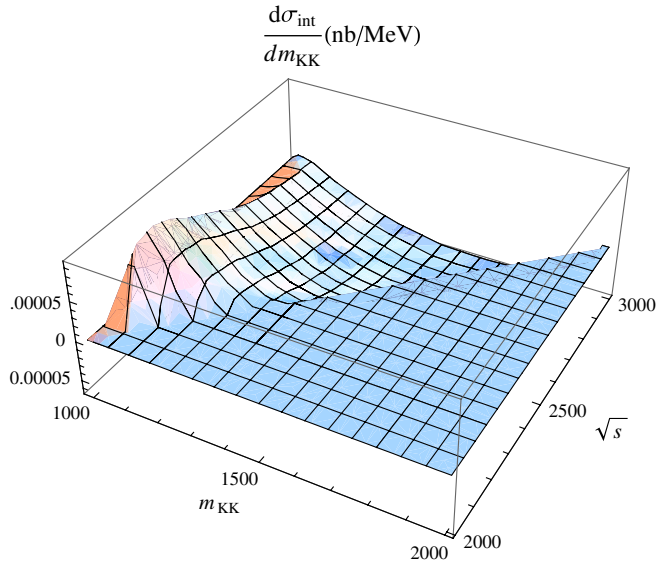

FIG. 11 (color online). Dikaon spectrum of the contributions coming from the interference between rescattering and tree level as a function of the dikaon invariant mass for different values of the center of mass energy.

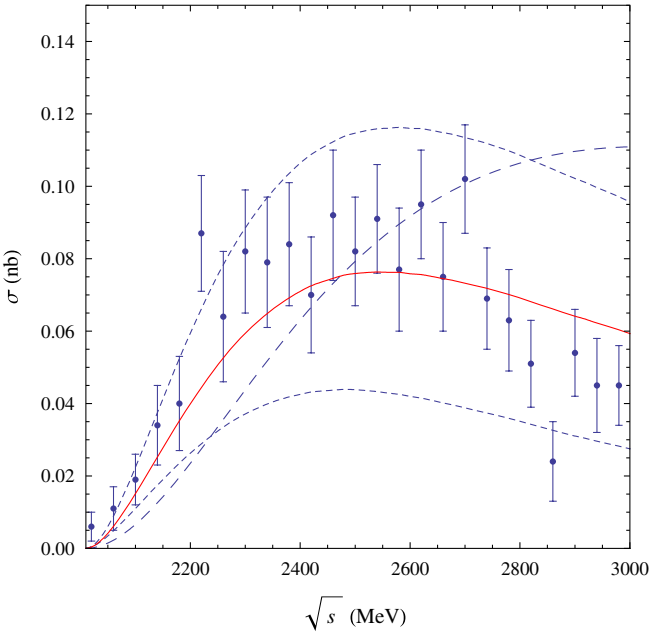

FIG. 12 (color online). Cross section for $e^+e^- \to \phi K^+K^-$ as a function of the center of mass energy (solid line). Short-dashed lines correspond to the 1σ region of the transition form factors in Figs. 5 and 6. The long-dashed line corresponds to tree-level contributions. The experimental points are taken from Ref. [3] and correspond to the cross section for $e^+e^- \to K^+K^-K^+K^-$ with one of the kaon pairs coming from a ϕ (see the discussion in the body of the paper).

close to the reaction threshold which evolves to a destructive interference beyond $\sqrt{s} = 1475$ MeV. In this figure our results are compared with measurements of the cross section for $e^+e^- \to K^+K^-K^+K^-$ from Ref. [3]. This comparison makes sense since, as shown in Fig. 25 of [3], for most of the considered events one of the final K^+K^- pairs comes from a ϕ. Using the narrow width approximation (quite appropriate for the ϕ) it can be shown that the measured cross section coincides with the cross section for $e^+e^- \to \phi K^+K^-$. In Fig. 12 we see that the interference between tree-level and rescattering effects is crucial in the proper description of data. Above 2700 MeV we expect higher l dikaon contributions (exchange of tensor mesons in the $K\bar{K}$ rescattering) not considered in the unitarized amplitudes which per construction are the $l = 0$ projected amplitudes.

In Ref. [2] the authors observed a peak, named $X(2175)$, around $\sqrt{s} = 2175$ MeV in the cross section of the $e^+e^- \to \phi\pi\pi$ with the dipion invariant mass in the $f_0(980)$ peak region. The $X(2175) \to \phi f_0$ mode was also observed at BES and BELLE thus the $X(2175)$ must be an isoscalar $J^{PC} = 1^{--}$ state. The mass and width measured in the $\phi f_0(980)$ channel, $M_X = 2175$ MeV, $\Gamma_X = 57$ MeV, disagree with the predictions of quark models for the 3^3S_1 state (e.g. [21] predicts $M_X^{QM} = 2050$ MeV, $\Gamma_X^{QM} = 378$ MeV), thus alternative structures have been

proposed for this resonance [22,23]. In particular, a narrow peak with a mass close to the experimental value has been generated solving the Faddeev equations for the three body problem involving chiral interactions of the $\phi K\bar{K}$ system [23]. The peak appears for a $K\bar{K}$ invariant mass close to the f_0 pointing to the $X(2175)$ as a ϕf_0 dynamically generated resonance. Clearly, there must exist contributions from the intermediate $X(2175)$ to $e^+e^- \to \phi K^+K^-$. Furthermore, since the K^+K^- system in this reaction can also be in an isovector state, in principle this reaction could get contributions from an isovector companion of the $X(2175)$ if it exists and in this concern it is worth remarking that in the approach of [23] no peak is generated in the isovector channel. Since our calculation accounts for most of the experimental data, we would expect these contributions to be small except perhaps around $\sqrt{s} = 2220$ MeV where there is a point out of the region obtained using the characterization of the K^*K transition form factors within 1σ. This point is slightly above the $X(2175)$ peak observed by *BABAR* and BES collaborations and could be a signal of intermediate resonances whose shape is distorted by their own interference and interference with the mechanisms studied here. In this concern it is desirable to have a rough estimate of the contributions of the intermediate $X(2175)$ via the chain $e^+e^- \to X \to \phi f_0 \to \phi K^+K^-$ with a slightly off-shell f_0. We devote the following section to the calculation of these contributions.

VII. INTERMEDIATE $X(2175)$ CONTRIBUTIONS

In Ref. [2], the product

$$\mathrm{BR}\,(X \to \phi f_0)\Gamma(X \to e^+e^-) = 2.5 \pm 0.8 \pm 0.4\ \mathrm{eV} \tag{55}$$

was obtained. This allows us to estimate the intermediate $X(2175)$ contributions depicted in Fig. 13. For the γX and $X\phi f_0$ interactions we use the phenomenological Lagrangians

$$\mathcal{L}_{X\gamma} = \frac{eG_{X\gamma}}{2}X^{\mu\nu}F_{\mu\nu}, \qquad \mathcal{L}_{X\phi f} = \frac{G_{X\phi f}}{2}X^{\mu\nu}\phi_{\mu\nu}f,$$
$$\mathcal{L}_{fK^+K^-} = G_{fK^+K^-}fK^+K^-. \tag{56}$$

From these interactions, in the corresponding center of momentum system (c.m.s.) we obtain

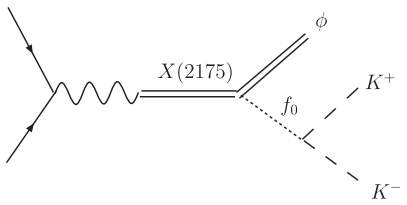

FIG. 13. Intermediate $X(2175)$ contributions to $e^+e^- \to \phi K^+K^-$.

$$\Gamma(X \to e^+e^-) = \frac{4\pi\alpha^2 G_{X\gamma}^2}{3M_X},$$
$$\Gamma(X \to \phi f_0) = \frac{G_{X\phi f}^2|\mathbf{p}_\phi|}{24\pi M_X^2}(2E_\phi^2 + M_\phi^2). \tag{57}$$

The amplitude for Fig. 13 reads

$$-i\mathcal{M}_L = ie^2 G_{X\phi f}G_{X\gamma}G_{fK^+K^-}\left(\frac{1}{s - M_X^2 + i\Gamma_X M_X}\right)$$
$$\times\left(\frac{1}{m_{KK}^2 - m_f^2 + i\Gamma_f m_f}\right)\frac{L^\mu}{k^2}L^{(1)}_{\mu\nu}\eta^\nu. \tag{58}$$

Using the *BABAR* central values $M_X = 2175$ MeV, $\Gamma_X = 57$ MeV, the product $G_{X\gamma}^2 G_{X\phi f}^2$ as extracted from Eqs. (55) and (57), $G_{fK^+K^-} = 3.76$ GeV [24], and the Particle Data Group values $m_f = 980$ MeV, $\Gamma_f = 40$ MeV [25] we obtain the cross section shown in Fig. 14. Close to the peak of the $X(2175)$ these contributions are of the same order as the ones previously considered thus they must be included in our calculation. The relative sign between this amplitude and the previous contributions cannot be fixed thus we explore both constructive and destructive interference. Our results are shown in Figs. 15 and 16, for constructive and destructive interference, respectively. In the case of constructive interference, our calculation suggests that the effects of the $X(2175)$ could be seen in $e^+e^- \to \phi K^+K^-$ over the background generated by the intermediate light vectors and the rescattring effects. In the case of destructive interference, a dip is generated instead of a peak and this seems to be the case favored by data. However, definite conclusions require a more precise extraction of the isovector K^*K transition form factor at $\sqrt{s} \approx 2$ GeV (see Fig. 6) because the tree-level intermediate light vectors and rescattering contributions are sensitive to this form factor. Indeed, using only

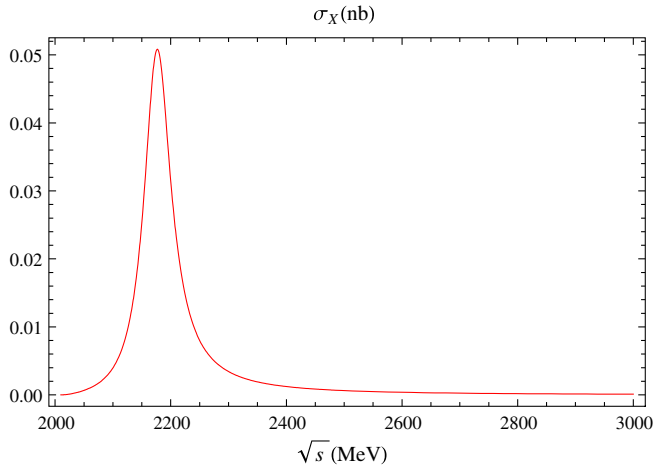

FIG. 14 (color online). Cross section for the intermediate $X(2175)$ contributions to $e^+e^- \to \phi K^+K^-$ as a function of the center of mass energy.

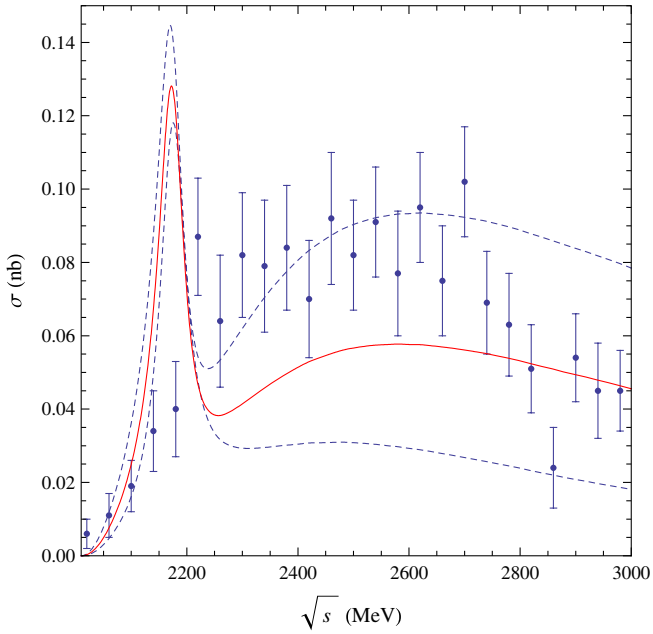

FIG. 15 (color online). Cross section for $e^+e^- \to \phi K^+K^-$ as a function of the center of mass energy including all contributions (solid line) and constructive interference. Short-dashed lines correspond to the 1σ region of the transition form factors in Figs. 5 and 6.

data in the 2–3 GeV region in the fit of the isovector form factor we obtain an increase of roughly 25% in the cross section shown in Figs. 15 and 16 with a similar energy dependence for $\sqrt{s} < 2.5$ GeV. Furthermore, intermediate contributions of a hypotetical isovector companion of the $X(2175)$ cannot be excluded at this point. The prediction of the absence of isovector companions of the $X(2175)$ in the framework of the dynamically generated resonances [23] makes it interesting to measure more accurately the cross section for $e^+e^- \to \phi K^+K^-$ in the near threshold region. The possible isovector resonance could be seen cleanly in the pure isovector $\phi\pi^0\eta$ final state thus we encourage experimentalists to measure also the $e^+e^- \to \phi\pi^0\eta$ cross section around $\sqrt{s} = 2.2$ GeV.

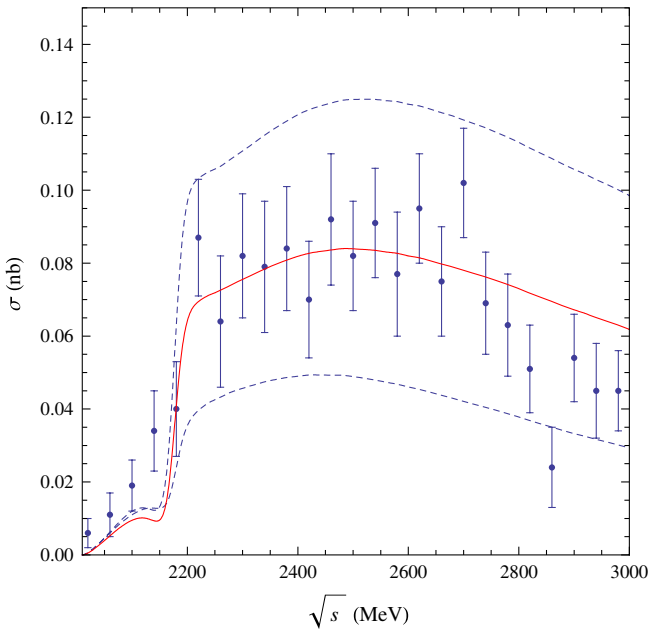

FIG. 16 (color online). Cross section for $e^+e^- \to \phi K^+K^-$ for destructive interference as a function of the center of mass energy including all contributions (solid line). Short-dashed lines correspond to the 1σ region of the transition form factors in Figs. 5 and 6.

VIII. SUMMARY AND CONCLUSIONS

We study electron-positron annihilation into ϕK^+K^-. We start with the $R\chi PT$ Lagrangian which yields tree-level contributions to this reaction involving both pseudoscalar and vector exchange. For the latter we use the conventional anomalous Lagrangian. The dynamics is dominated by the kaon form factors and the K^*K transition form factors, whose lowest order terms (valid for low photon virtualities), arise in the calculation with the effective theory. This result is improved replacing the lowest order terms provided by $R\chi PT$ for the kaon form factors, by the full form factor as calculated in $U\chi PT$ [14]. The K^*K transition form factors are extracted from recent data on $e^+e^- \to K^*K$ [18] and used in the numerics instead of the lowest order terms arising from the anomalous $VV'P$ Lagrangian.

We consider also rescattering of the final charged kaons and ϕK^+K^- production through intermediate $\phi K^0\bar{K}^0$ production and subsequent rescattering $K^0\bar{K}^0 \to K^+K^-$. The corresponding results, valid for low energy dikaon mass are improved using the unitarized meson-meson amplitudes containing the scalar poles [12] instead of the lowest order terms obtained in the calculation with χPT.

The dynamical generation of the scalar resonances in the meson-meson unitarized amplitudes enhances the rescattering effects close to the reaction threshold. The poles of the scalar resonances lie below the dikaon threshold energy but the tail of the $f_0(980)$ and $a_0(980)$ mesons are visible in the dikaon spectrum of rescattering contributions. In spite of this, beyond the close to threshold region, the tree-level vector exchange contribution turns out to be dominant.

The calculated cross section is sensitive to the K^*K form factors but within 1σ in their fit to $e^+e^- \to K^*K$ recent data, we obtain results in agreement with measurements of the cross section for $e^+e^- \to K^+K^-K^+K^-$, where one of the kaon pairs comes from the decay of a ϕ, except in a narrow region near $\sqrt{s} = 2220$ MeV.

Since the $X(2175)$ has been observed in the $e^+e^- \to \phi f_0(980)$ reaction, and the $f_0(980)$ couples strongly to the K^+K^- system, the $X(2175)$ could also show up in the cross section for $e^+e^- \to \phi K^+K^-$ slightly beyond the threshold energy of the reaction in spite of the fact that it is not possible to see the whole $f_0(980)$ shape in the dikaon

invariant mass because it lies below the kinematical threshold for the production of two kaons. We estimate these contributions using phenomenological Lagrangians and extracting the product of the $X\gamma$ and $X\phi f_0$ couplings from the *BABAR* value for $\mathrm{BR}(X \to \phi f_0)\Gamma(X \to e^+e^-)$. We obtain a sizable contribution of intermediate $X(2175)$ to the $e^+e^- \to \phi K^+K^-$ at the $X(2175)$ peak.

Including all contributions we get the results as shown in Figs. 15 and 16. The large uncertainties in the extraction of the isovector K^*K transition form factor from data do not allow for definite conclusions but the data around $\sqrt{s} =$ 2220 MeV hints to a destructive interference between the intermediate $X(2175)$ contributions and to possible contributions from an isovector companion of the $X(2175)$. In the light of a recent calculation of the $X(2175)$ as a three body structure where no isovector companion is generated [23], it is important to have more precise data on the isovector K^*K transition form factor and on the cross section for $e^+e^- \to \phi K^+K^-$ near threshold. A cleaner signal of a hypothetical isovector companion of the $X(2175)$ could be detected in a pure isovector final state and in this concern it is worthy to study the $\phi\pi^0\eta$ channel from both the experimental and theoretical point of view.

ACKNOWLEDGMENTS

This work was partly supported by DGICYT Contract No. FIS2006-03438 and the Generalitat Valenciana. This research is part of the EU Integrated Infrastructure Initiative Hadron Physics Project under Contract No. RII3-CT-2004-506078. The work of M. Napsuciale was also supported by DINPO-UG and CONACyT-México under Project No. CONACyT-50471-F. Selim Gómez-Avila wishes to acknowledge support by CONACyT-México under the Mixed Grants Program. M. N. and S. G. wish to thank the hospitality of the theory group at IFIC. We thank E. P. Solodov for useful mail exchange concerning data presented in [3].

APPENDIX

The differential cross section is given by

$$d\sigma = \frac{(2\pi)^4|\bar{\mathcal{M}}|^2}{4\sqrt{(p_+\cdot p_-)^2 - m_e^4}}\delta^4(p_+ + p_- - Q - p - p') \times \frac{d^3Q}{(2\pi)^3 2\omega}\frac{d^3p}{(2\pi)^3 2E}\frac{d^3p'}{(2\pi)^3 2E'}. \quad \text{(A1)}$$

Integrating K^- variables we obtain

$$d\sigma = \frac{1}{(2\pi)^5}\frac{|\bar{\mathcal{M}}|^2}{4\sqrt{(p_+\cdot p_-)^2 - m_e^4}} \times \delta((p_+ + p_- - Q - p)^2 - m_K^2)\frac{d^3Q}{2\omega}\frac{d^3p}{2E}. \quad \text{(A2)}$$

Next we integrate the K^+ variables. We work in the center of momentum system (CMS). The kinematical constriction in this frame reads

$$(k - Q - p)^2 - m_K^2 = s + M_\phi^2 - 2\sqrt{s}(\omega + E) + 2(\omega E - |\mathbf{Q}||\mathbf{p}|\cos\theta) = 0, \quad \text{(A3)}$$

where $Q = (\omega, \mathbf{Q})$, $p = (E, \mathbf{p})$, and $\theta = \sphericalangle(\mathbf{Q}, \mathbf{p})$. In order to directly integrate the K^+ variables we choose our frame as shown in Fig. 17. With these conventions the $\phi - K^+$ angle θ is the K^+ polar angle and can be integrated using the δ function to obtain

$$d\sigma = \frac{1}{(2\pi)^5}\frac{|\bar{\mathcal{M}}|^2}{16s}d\omega d\Omega_Q dE d\varphi, \quad \text{(A4)}$$

where we neglected m_e terms in the flux factor.

The squared amplitude $|\bar{\mathcal{M}}|^2$ is a function of the scalar products of

$$p_-, \quad k, \quad Q, \quad l \equiv p - p'. \quad \text{(A5)}$$

Momentum conservation requires

$$n \equiv p + p' = k - Q. \quad \text{(A6)}$$

Furthermore $l \cdot n = 0$ thus

$$l \cdot k = l \cdot Q, \quad \text{(A7)}$$

hence the squared amplitude for this process in general depends only on the following scalar products:

$$l\cdot p_-, \quad l\cdot k, \quad l^2, \quad Q\cdot k, \quad Q\cdot p_-, \quad k\cdot p_-. \quad \text{(A8)}$$

The momentum $l = 2p - n = 2p - k + Q$ thus

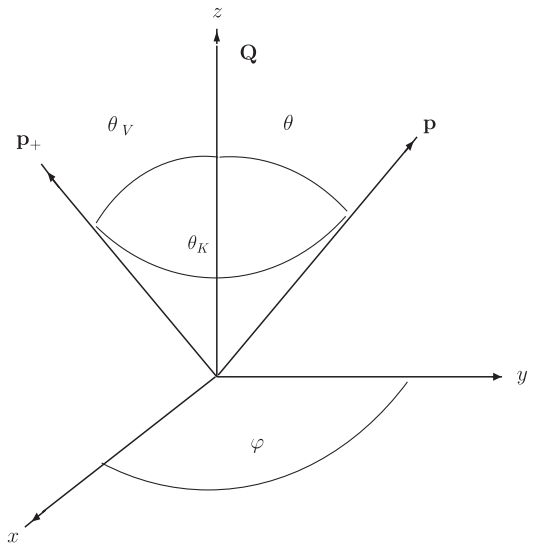

FIG. 17. Angle conventions.

$$l\cdot k=(2E-\sqrt{s}+\omega)\sqrt{s},$$

$$l\cdot p_-=-\frac{s}{2}+\sqrt{s}(E-|\mathbf{p}|\cos\theta_K)+\frac{\sqrt{s}}{2}(\omega-|\mathbf{Q}|\cos\theta_V),$$

$$l^2=4m^2-s-M_\phi^2+2\sqrt{s}\omega,\qquad Q\cdot k=\sqrt{s}\omega,$$

$$Q\cdot p_-=\frac{\sqrt{s}}{2}(\omega-|\mathbf{Q}|\cos\theta_V),\qquad k\cdot p_-=\frac{s}{2}.$$

Integration of φ requires the explicit form of the average squared amplitude since the dependence on $p_-\cdot p$ introduces a dependence on $\cos\theta_K$. Here we must take into account that this angle is related to the K^+-beam angle θ_K and the ϕ-beam angle θ_V as

$$\cos\theta_K=\cos\theta\cos\theta_V+\sin\theta\sin\theta_V\cos\phi, \tag{A9}$$

thus there is a nontrivial dependence on φ. The integration of the azimuthal angle of the ϕ is straightforward. Then we integrate the polar angle of the ϕ. Integration on E requires calculating the maximum and minimum kaon energy allowed by the kinematical constraint

$$s+M_\phi^2-2\sqrt{s}(\omega+E)+2(\omega E-|\mathbf{Q}||\mathbf{p}|\cos\theta)=0 \tag{A10}$$

for $\theta=0,\ \pi$, respectively. These are the solutions to

$$(s+M_\phi^2-2\sqrt{s}\omega-2(\sqrt{s}-\omega)E)^2=4(\omega^2-M_\phi^2)(E^2-m_K^2) \tag{A11}$$

which turn out to be

$$E_\pm=\frac{1}{2}\left[(\sqrt{s}-\omega)\pm\omega\sqrt{\left(1-\frac{M_\phi^2}{\omega^2}\right)\left(1-\frac{4m_K^2}{(s+M_\phi^2-2\sqrt{s}\omega)}\right)}\right]. \tag{A12}$$

This way we get the spectrum

$$\frac{d\sigma}{d\omega}=\frac{1}{(2\pi)^4}\frac{1}{16s}\int_{E_-}^{E_+}dE\int_0^\pi d\cos\theta_V\int_0^{2\pi}d\varphi|\bar{\mathcal{M}}|^2. \tag{A13}$$

This spectrum can be written in terms of the dikaon invariant mass related to ω and $\mathbf{Q}$ as

$$\omega=\frac{s+M_\phi^2-m_{KK}^2}{2\sqrt{s}},\qquad |\mathbf{Q}|=\frac{\lambda^{1/2}(s,m_K^2,m_{KK}^2)}{2\sqrt{s}} \tag{A14}$$

with the function λ defined in Eq. (49). The dikaon spectrum is

$$\frac{d\sigma}{dm_{KK}}=\frac{1}{(2\pi)^4}\frac{m_{KK}}{16s^{3/2}}\times\int_{E_-}^{E_+}dE\int_0^\pi d\cos\theta_V\int_0^{2\pi}d\varphi|\bar{\mathcal{M}}|^2.$$

It is convenient to work with the dimensionless quantities

$$x=\frac{2\omega}{\sqrt{s}},\quad y=\frac{2E}{\sqrt{s}},\quad \xi=\frac{4m_K^2}{s},\quad \chi=\frac{M_\phi^2}{s},\quad \rho=\frac{m_{KK}}{s}. \tag{A15}$$

In terms of these quantities

$$\cos\theta=\frac{xy}{\sqrt{x^2-4\chi}\sqrt{y^2-\xi}}\left(1+\frac{2(1+\chi-x-y)}{xy}\right),$$

$$y_\pm=1-\frac{x}{2}\pm\frac{x}{2}\sqrt{\left(1-\frac{4\chi}{x^2}\right)\left(1-\frac{\xi}{(1-x+\chi)}\right)}.$$

In terms of these variables the scalar products read

$$l\cdot k=\frac{s}{2}(x+2y-2),$$

$$l\cdot p_-=\frac{s}{2}\left(-1+\frac{x}{2}+y-\sqrt{y^2-\xi}\cos\theta_K-\frac{1}{2}\sqrt{x^2-4\chi}\cos\theta_V\right),$$

$$l^2=s(\xi-\chi+x-1),\qquad Q\cdot k=\frac{s}{2}x,$$

$$Q\cdot p_-=\frac{s}{4}(x-\sqrt{x^2-4\chi}\cos\theta_V),\qquad k\cdot p_-=\frac{s}{2}.$$

The range of values for ω are $\omega_{\min}=M_\phi$, $\omega_{\max}=(s+M_\phi^2-4m_K^2)/2\sqrt{s}$ thus

$$x_{\min}=2\sqrt{\chi},\qquad x_{\max}=1+\chi-\xi. \tag{A16}$$

[1] M. Benayoun, S. I. Eidelman, V. N. Ivanchenko, and Z. K. Silagadze, Mod. Phys. Lett. A **14**, 2605 (1999); A. Denig, Nucl. Phys. B, Proc. Suppl. **162**, 81 (2006); D. Leone (KLOE Collaboration), Nucl. Phys. B, Proc. Suppl. **162**, 95 (2006); H. Czyz, A. Grzelinska, J. H. Kuhn, and G. Rodrigo, Eur. Phys. J. C **47**, 617 (2006); A. G. Denig (KLOE Collaboration), Int. J. Mod. Phys. A **20**, 1935 (2005); J. H. Kuhn, Eur. Phys. J. C **33**, S659 (2004); S. E. Muller (KLOE Collaboration), Nucl. Phys. B, Proc. Suppl. **126**, 335 (2004); A. G. Denig *et al.* (KLOE Collaboration), Nucl. Phys. B, Proc. Suppl. **116**, 243 (2003); B. Aubert *et al.* (*BABAR* Collaboration), Phys. Rev. D **70**, 072004 (2004); ()**71**, 052001 (2005); ()**73**, 012005 (2006); ()**73**, 052003 (2006); R. Baldini Ferroli (*BABAR* Collaboration), Int. J. Mod. Phys. A **21**, 5565 (2006); B. A. Shwartz (Belle Collaboration), Nucl. Phys.

B, Proc. Suppl. **144**, 245 (2005); H. Czyz, A. Grzelinska, J. H. Kuhn, and G. Rodrigo, Eur. Phys. J. C **39**, 411 (2005); H. Czyz, J. H. Kuhn, E. Nowak, and G. Rodrigo, Eur. Phys. J. C **35**, 527 (2004); H. Czyz, A. Grzelinska, J. H. Kuhn , and G. Rodrigo, Eur. Phys. J. C **27**, 563 (2003).

[2] B. Aubert *et al.* (*BABAR* Collaboration), Phys. Rev. D **74**, 091103 (2006).

[3] B. Aubert *et al.* (*BABAR* Collaboration), Phys. Rev. D **76**, 012008 (2007).

[4] M. Ablikim *et al.* (BES Collaboration), Phys. Rev. Lett. **100**, 102003 (2008).

[5] I. Adachi *et al.* (Belle Collaboration), arXiv:0808.0006.

[6] V. M. Aulchenko *et al.* (SND Collaboration), Phys. Lett. B **440**, 442 (1998); R. R. Akhmetshin *et al.* (CMD-2 Collaboration), Phys. Lett. B **462**, 380 (1999); A. Aloisio *et al.* (KLOE Collaboration), Phys. Lett. B **537**, 21 (2002); F. Ambrosino *et al.* (KLOE Collaboration), Eur. Phys. J. C **49**, 473 (2007); F. Ambrosino *et al.* (KLOE Collaboration), Phys. Lett. B **634**, 148 (2006).

[7] A. Bramon, R. Escribano, J. L. Lucio, M. M. Napsuciale, and G. Pancheri, Eur. Phys. J. C **26**, 253 (2002); D. Black, M. Harada, and J. Schechter, Phys. Rev. D **73**, 054017 (2006); D. Black, M. Harada, and J. Schechter, Phys. Rev. Lett. **88**, 181603 (2002).

[8] E. Marco, S. Hirenzaki, E. Oset, and H. Toki, Phys. Lett. B **470**, 20 (1999); V. E. Markushin, Eur. Phys. J. A **8**, 389 (2000); J. E. Palomar, L. Roca, E. Oset, and M. J. Vicente Vacas, Nucl. Phys. **A729**, 743 (2003); J. A. Oller, Nucl. Phys. **A714**, 161 (2003).

[9] M. Napsuciale, E. Oset, K. Sasaki, and C. A. Vaquera-Araujo, Phys. Rev. D **76**, 074012 (2007).

[10] Yu. M. Bystritskiy, M. K. Volkov, E. A. Kuraev, E. Bartos, and M. Secansky, Phys. Rev. D **77**, 054008 (2008).

[11] G. Ecker, J. Gasser, A. Pich, and E. de Rafael, Nucl. Phys. **B321**, 311 (1989).

[12] J. A. Oller and E. Oset, Nucl. Phys. **A620**, 438 (1997) **A652**, 407(E) (1999).

[13] J. A. Oller, E. Oset, and J. R. Pelaez, Phys. Rev. Lett. **80**, 3452 (1998); J. A. Oller, E. Oset, and J. R. Pelaez, Phys. Rev. D **59**, 074001 (1999); **60**, 099906(E) (1999).

[14] J. A. Oller, E. Oset, and J. E. Palomar, Phys. Rev. D **63**, 114009 (2001); J. A. Oller and E. Oset, Phys. Rev. D **60**, 074023 (1999).

[15] D. Bisello *et al.* (DM2 Collaboration), Z. Phys. C **39**, 13 (1988); B. Delcourt, D. Bisello, J. C. Bizot, J. Buon, A. Cordier, and F. Mane, Phys. Lett. B **99**, 257 (1981).

[16] F. Mane, D. Bisello, J. C. Bizot, J. Buon, A. Cordier, and B. Delcourt, Phys. Lett. B **99**, 261 (1981).

[17] D. Bisello *et al.*, Z. Phys. C **52**, 227 (1991); F. Mane, D. Bisello, J. C. Bizot, J. Buon, A. Cordier, and B. Delcourt, Phys. Lett. B **112**, 178 (1982).

[18] B. Aubert *et al.* (*BABAR* Collaboration), Phys. Rev. D **77**, 092002 (2008).

[19] G. Ecker, J. Gasser, H. Leutwyler, A. Pich, and E. de Rafael, Phys. Lett. B **223**, 425 (1989).

[20] U. G. Meissner and J. A. Oller, Nucl. Phys. **A679**, 671 (2001); A. Falvard *et al.* (DM2 Collaboration), Phys. Rev. D **38**, 2706 (1988); M. Ablikim *et al.* (BES Collaboration), Phys. Lett. B **607**, 243 (2005); J. Z. Bai *et al.* (BES Collaboration), Phys. Rev. D **68**, 052003 (2003).

[21] T. Barnes, N. Black, and P. R. Page, Phys. Rev. D **68**, 054014 (2003).

[22] G. J. Ding and M. L. Yan, Phys. Lett. B **650**, 390 (2007); G. J. Ding and M. L. Yan, Phys. Lett. B **657**, 49 (2007); Z. G. Wang, Nucl. Phys. **A791**, 106 (2007); H. X. Chen, X. Liu, A. Hosaka, and S. L. Zhu, Phys. Rev. D **78**, 034012 (2008).

[23] A. Martinez Torres, K. P. Khemchandani, L. S. Geng, M. Napsuciale, and E. Oset, Phys. Rev. D **78**, 074031 (2008).

[24] F. Ambrosino *et al.* (KLOE Collaboration), Eur. Phys. J. C **49**, 473 (2007).

[25] C. Amsler *et al.*, Phys. Lett. B **667**, 1 (2008).